Available online at www.sciencedirect.com
ScienceDirect
International Journal of Fatigue 29 (2007) 931–940
International Journal of Fatigue
www.elsevier.com/locate/ijfatigue

Statistical modeling of fatigue crack growth rate in Inconel alloy 600

Kassim S. Al-Rubaie [a], Leonardo B. Godefroid [b,*], Jadir A.M. Lopes [c]

[a] EMBRAER (Empresa Brasileira de Aeronáutica), Av. Brigadeiro Faria Lima 2170, 12227-901 São José dos Campos, SP, Brazil
[b] Universidade Federal de Ouro Preto, Escola de Minas, Dept. de Engenharia Metalúrgica e de Materiais, Praça Tiradentes 20, 35400-000 Ouro Preto, MG, Brazil
[c] Centro de Desenvolvimento da Tecnologia Nuclear – CDTN/CNEN Cidade Universitária, Pampulha, 30123-970 Belo Horizonte, MG, Brazil

Received 29 December 2005; received in revised form 24 July 2006; accepted 30 July 2006
Available online 26 September 2006

Abstract

Inconel alloy 600 is widely used in heat-treating industry, in chemical and food processing, in aeronautical industry, and in nuclear engineering. In this work, fatigue crack growth rate (FCGR) was evaluated in air and at room temperature under constant amplitude loading at a stress ratio of 0.1, using compact tension specimens. Collipriest and Priddle FCGR models were proposed to model the data. In addition, these models were modified to obtain a better fit to the data, especially in the near-threshold region. Akaike information criterion was used to select the candidate model that best approximates the real process given the data. The results showed that both Collipriest and Priddle models fit the FCGR data in a similar fashion. However, the Priddle model provided better fit than the Collipriest model. The modified Priddle model was found to be the most appropriate model for the data.

Keywords: Inconel alloy 600; Fatigue crack growth rate; Statistical modeling; Nonlinear regression; Model selection; Akaike information criterion

1. Introduction

Inconel alloy 600 is a nickel–chromium–iron superalloy (Ni–Cr–Fe) that is widely used because of its good corrosion and oxidation resistance [1–3]. This is a solid solution strengthened alloy, normally used in the annealed temper; the annealing treatment is dependent on properties required by the application. The alloy has good mechanical properties and presents the desirable combination of strength and toughness. The high nickel content of the alloy enables it to resist corrosion caused by many organic and inorganic compounds and also gives it high resistance to chloride ion stress corrosion cracking. The chromium content provides a resistance to sulfur compounds and to various oxidizing environments at high temperatures or in corrosive solutions [1,4].

Inconel alloy 600 is widely used in a variety of applications. For its strength and corrosion resistance, it is used extensively in the chemical industry. Due to its strength and oxidation resistance at high temperatures, it is used for many applications in the heat-treating industry. In the aeronautical field, this alloy is used for a variety of engine and airframe components that must withstand high temperatures. Inconel alloy 600 is the standard material for construction of nuclear reactors. It has excellent resistance to high-purity water. Moreover, it is very resistant to chloride ion stress corrosion cracking in reactor water systems [5].

Tubes of a pressurized water reactor (PWR) steam generator of a nuclear power plant represent the majority of the reactor coolant pressure boundary. The flow of cooling water with high velocity can cause cycling stresses (e.g. thermal cycling and vibration) in the tubes, generally made of Inconel alloys 600 and 690. The stresses may initiate and propagate fatigue cracks. In addition, aggressive service environments often accelerate the degradation rate. Excessive degradation may lead to failure of tubes and therefore

* Corresponding author. Tel.: +55 31 3551 3012/3551 1586; fax: +55 31 3551 3012.
E-mail address: leonardo@demet.em.ufop.br (L.B. Godefroid).

0142-1123/$ - see front matter © 2006 Elsevier Ltd. All rights reserved.
doi:10.1016/j.ijfatigue.2006.07.013

implies reduced availability and safety of the entire plant [6].

The objective of this study is to present and model FCGR data of Inconel alloy 600 at room temperature, since few works [7–10] have been published. Due to the sigmoidal shape of the log(da/dN)–log(ΔK) curve, Collipriest [11,12] and Priddle [13] models were chosen to model the data. These models fit the entire FCGR curve. Nonlinear statistical analysis [14,15] was done to estimate model parameters. Akaike information criterion [16–19] was used to select the most appropriate model to the data.

2. Experimental procedure

Inconel alloy 600 with a thickness of 7 mm was used. The chemical composition is shown in Table 1.

Light microscopy was carried out on samples, polished with 1 μm diamond paste and electrochemically etched with a solution of 10% phosphoric acid. Grain size measurement was done using a computerised image analysis. Vickers hardness test was performed with a load of 196 N for a time of 30 s. According to ASTM E8 [20], tensile test was carried out with a rate of 2 mm/min using a 100 kN Instron machine.

FCGR test was conducted on pre-cracked compact tension specimens in accordance with ASTM E 647 [21]. The test was done under a constant amplitude sinusoidal wave loading at a stress ratio (R) of 0.1 using a 100 kN MTS servo-hydraulic machine, interfaced to a computer for machine control and data acquisition. The test was done at a frequency of 30 Hz under room temperature conditions that ranged from 20 °C to 25 °C with a relative humidity from 60% to 70% in air. The crack length was measured using a compliance method, in which a clip gauge is used to measure the elastic compliance of the specimen, which tends to increase with crack growth.

In addition, fatigue crack growth threshold (ΔK_{th}) was evaluated using a "load shedding" method proposed in ASTM E647 [21]. Basically, the test was conducted where the stress intensity factor range ($\Delta K = K_{max} - K_{min}$) was decreased. Consequently, crack growth slowed down and the threshold was reached as the crack stopped growing, or reached a sufficiently low FCGR. According to ASTM E647, ΔK_{th} is about the ΔK corresponding to a FCGR (da/dN) of 10^{-10} m/cycle.

Fracture toughness was evaluated by the R-curve determination at room temperature and in air environment using compact tension specimens, in accordance with ASTM E561 [22]. Basically, cyclic loading was applied to introduce a fatigue crack. As the crack reached the desired length, the fatigue cycling was stopped, and the load was gradually increased until fracture occurred. The stress intensity K_c is the value of K_R at the instability condition determined from the tangency point between the R-curve and one of the applied K-curves.

Fracture surfaces were analyzed in a JEOL scanning electron microscope.

Table 1
Chemical composition of Inconel alloy 600 (wt.%)

C	S	Fe	Cr	Ni
0.070	0.0007	9.46	13.92	70.12

3. Results and discussion

3.1. Microstructure and mechanical behaviour

Fig. 1 reveals the microstructure of the alloy with heterogeneous grains. The average grain size was determined as 14 μm with a standard deviation of 9 μm.

The results of the mechanical properties are presented in Table 2. They met the specifications described in AMS 5540L [23].

Fractographic analysis of tensile and fracture toughness specimens showed a transgranular and ductile fracture, with a mechanism of void nucleation, growth and coalescence. Fig. 2 shows this behaviour.

Fractographic analysis of fatigue crack growth at near-threshold shows a predominant transgranular fracture mode, with the "hill-and-valley" type appearance and shear facets, with an associated zig-zag path (Fig. 3a). Such fracture demonstrates high roughness and high crack deflection angles, characteristic of extensive crack closure induced by asperity wedging. At higher growth rates, fracture surfaces remain transgranular, but with evidence of striations (Fig. 3b).

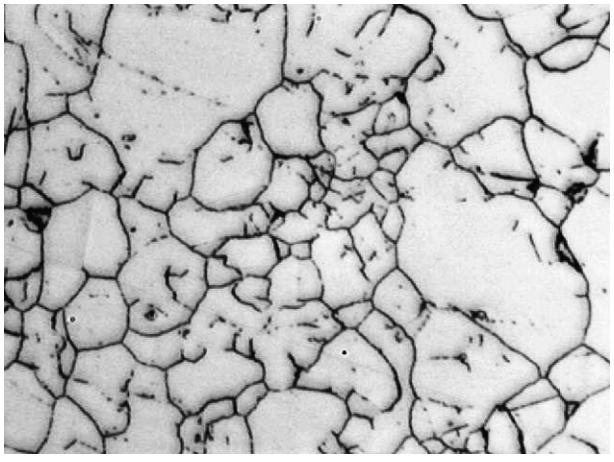

Fig. 1. Microstructure of Inconel alloy 600, electrochemical etching, 10% phosphoric acid, (400×).

Table 2
Room temperature mechanical properties of Inconel alloy 600

σ_{YS}, MPa	σ_{TS}, MPa	ε, %	Hardness, HV	K_c, MPa$\sqrt{m}$	ΔK_{th}, MPa$\sqrt{m}$
386	687	33.5	224	40.08	6.38

σ_{YS}: 0.2% yield tensile strength; σ_{TS}: ultimate tensile strength; ε: total strain; K_c: critical stress intensity factor (fracture toughness); ΔK_{th}: threshold stress intensity factor range.

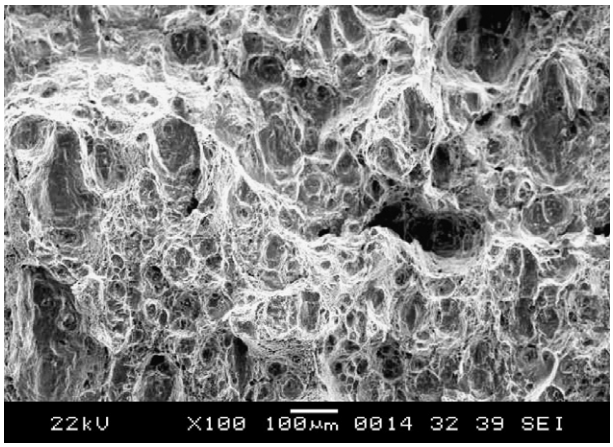

Fig. 2. SEM fractography of toughness specimen of the Inconel alloy 600, 100×.

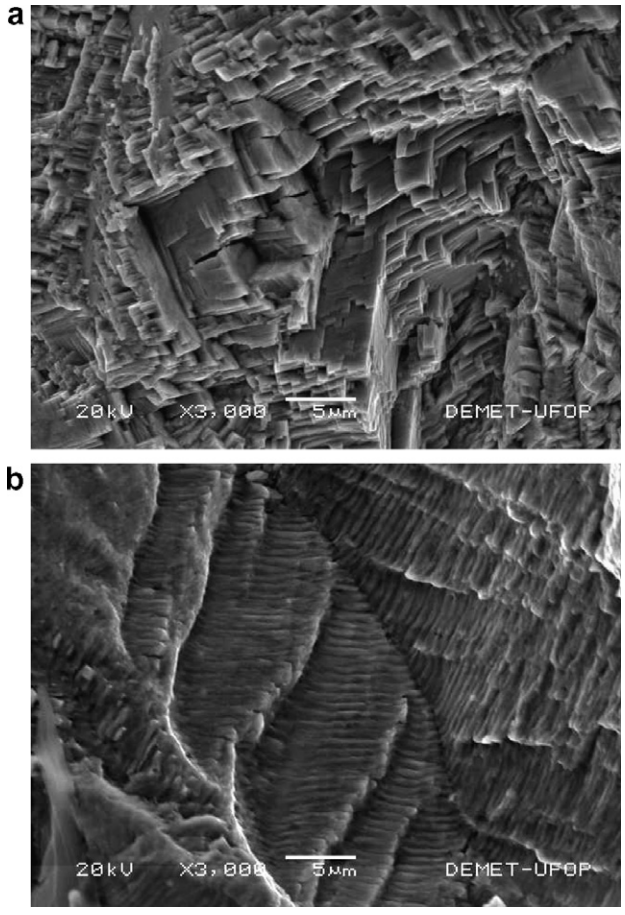

Fig. 3. SEM fractography of fatigue surface of the Inconel alloy 600, 3000×. (a) At the near-threshold region, and (b) at higher crack growth rate.

3.2. FCGR modeling

3.2.1. FCGR models

The reason for building models is to link theoretical ideas with the observed data to provide a good prediction of future observations. Modeling of FCGR data has enhanced the ability to create damage tolerant design philosophies. Paris and Erdogan [24] proposed the most important and popular work. They were the first who correlated FCGR with fracture mechanics parameters (K_{min} and K_{max}), describing the loading conditions in the region of the crack front. They observed a linear relationship between FCGR (da/dN) and ΔK when plotted on a log–log scale. Paris and Erdogan proposed the power law relationship:

$$\frac{da}{dN} = C\Delta K^n \tag{1}$$

where C and n are material parameters estimated from experimental data.

The Paris–Erdogan equation does not consider: (a) the effect of R, (b) the existence of ΔK_{th}, and (c) the accelerated FCGR when the maximum stress intensity factor (K_{max}) approaches the fracture toughness (K_c). It does not adequately describe FCGR regions I and III; it tends to overestimate region I and underestimate region III. Although the Paris–Erdogan equation is a simplification of a very complex phenomenon, it is still very popular on account of significant engineering interest.

The typical curve of a $\log(da/dN)$–$\log(\Delta K)$, at a prescribed condition (environment and R), is sigmoidal in shape. It comprises three regions and is bounded at its extremes by ΔK_{th} and ΔK_c. In the intermediate region of the curve, there is a linear relation between $\log(da/dN)$ and $\log(\Delta K)$, as proposed by Paris and Erdogan.

Based on Eq. (1), many FCGR models have been suggested to fit all or part of the sigmoidal curve. In this study, two models that fit all parts of FCGR curve are considered. These models are:

1. Collipriest model
   Collipriest suggests the following inverse hyperbolic tangent function [11,12]:

$$\frac{da}{dN} = C(K_c\Delta K_{th})^{\frac{n}{2}} \times \exp\left[\ln\left(\frac{K_c}{\Delta K_{th}}\right)^{\frac{n}{2}} \tanh^{-1}\frac{\ln\left(\frac{\Delta K^2}{\Delta K_{th}K_c(1-R)}\right)}{\ln\left(\frac{K_c(1-R)}{\Delta K_{th}}\right)}\right] \tag{2}$$

   where ln denotes the natural logarithm.
2. Priddle model
   Priddle proposed the following function [13]:

$$\frac{da}{dN} = C\left(\frac{\Delta K - \Delta K_{th}}{K_c - K_{max}}\right)^n \tag{3}$$

   Since $\Delta K = K_{max}(1-R)$, the model is given by

$$\frac{da}{dN} = C\left(\frac{\Delta K(1-R) - \Delta K_{th}(1-R)}{K_c(1-R) - \Delta K}\right)^n \tag{4}$$

Based on the results presented in [25], both Collipriest and Priddle models are modified by adding an extra parameter (m) to obtain a better fit to the data, especially in the

near-threshold region. The modified models are given respectively by Eqs. (5) and (6).

$$\frac{da}{dN} = C(K_c \Delta K_{th})^{\frac{n}{2}} \times \exp\left[\ln\left(\frac{K_c}{\Delta K_{th}}\right)^{\frac{n}{2}} \tanh^{-1} \frac{\ln\left(\frac{\Delta K^2}{\Delta K_{th} K_c (1-mR)}\right)}{\ln\left(\frac{K_c(1-R)}{\Delta K_{th}}\right)}\right] \quad (5)$$

$$\frac{da}{dN} = C\left(\frac{\Delta K(1-R) - \Delta K_{th}(1-mR)}{K_c(1-R) - \Delta K}\right)^n \quad (6)$$

3.2.2. Model fitting

Collipriest and Priddle models and their modifications are nonlinear regression models. A nonlinear model has at least one parameter (quantity to be estimated) that appears nonlinearly [14,15]. Nonlinear regression is an iterative procedure, and the basis used for estimating the unknown parameters is the criterion of least-squares. The fitting was carried out using a routine based on the Marquardt–Levenberg algorithm [26]. The fitting procedure provides: (i) parameters, (ii) error estimate on the parameter, and (iii) a statistical measure of goodness of fit.

The estimated parameters and the statistical properties for FCGR models are presented in Tables 3 and 4. At the 0.05 and 0.01 levels of significance, the estimated parameters are statistically significant, since their *p-values* are smaller than the levels of significance.

The experimental data and the estimated curves are shown in Figs. 4–6. The visual examination of these curves reveals that the modification in the Collipriest model provides a better fit (Fig. 4). The same is also true for the case of the modified Priddle model (Fig. 5). In addition, the modified Priddle model provides a better fit than the modified Collipriest (Fig. 6). It implies that the modified Priddle model offers the best approximation of the data.

3.2.3. Model validation

There are various graphical and numerical tools to assist goodness of fit of a model used with experimental data [27,28]. The most common approach is to examine the residual. Three forms of graphical analysis were used. These are:

3.2.3.1. Measured–predicted plot. Plots of measured FCGR against predictions of the underlying models are shown in Fig. 7. The straight line gives values for measured = predicted. An advantage of this type of plot is that the vertical deviations from the line are the actual residuals from the full fit. A residual is positive if the corresponding data point lies above the line and negative if the point lies below the line. Collipriest and Priddle models (Fig. 7a and b) behave in a similar fashion; it is hard to distinguish between them. The same is also true when the modified Collipriest and modified Priddle models are compared; however, the latter has relatively more support in the data, where the data points come close to the theoretical solid line.

3.2.3.2. Box plot. Box plot provides a graphical display of data based on five-number summary (smallest value, lower quartile ($Q1$), median, upper quartile ($Q3$), and largest value). In box plot with a vertical orientation, $Q1$ and $Q3$ of the data are the lower and the upper lines of the box. The interquartile range (IQR) is the difference between

Table 3
Estimated parameters of FCGR models, Inconel alloy 600, $R = 0.1$

Model	Parameter	Estimate	Std. error	*t*-Value	*p*-Value	95% LCL	95% UCL
Collipriest	C	5.609E−12	7.023E−13	7.987	3.76E−11	4.206E−12	7.012E−12
	n	2.621	4.809E−02	54.508	<2E−16	2.525	2.718
Priddle	C	2.454E−08	1.015E−09	24.176	<2E−16	2.252E−08	2.657E−08
	n	1.151	2.034E−02	56.60	<2E−16	1.111	1.192
Modified Collipriest	C	2.657E−12	3.300E−13	8.051	3.23E−11	1.997E−12	3.317E−12
	n	2.772	3.798E−02	72.980	<2E−16	2.696	2.848
	m	2.301	1.892E−01	12.161	<2E−16	1.923	2.679
Modified Priddle	C	2.425E−08	7.425E−10	32.658	<2E−16	2.276E−08	2.573E−08
	n	1.394	3.768E−02	36.996	<2E−16	1.318	1.469
	m	2.463	2.592E−01	9.506	1.02E−13	1.945	2.981

Table 4
Statistical properties of FCGR models, Inconel alloy 600, $R = 0.1$

Model	SSE	SE	MSE	R^2	R^2_{adj}
Collipriest	0.63614	0.10049	0.01010	0.9792	0.9789
Priddle	0.59086	0.09684	0.00938	0.9807	0.9804
Modified Collipriest	0.34415	0.07450	0.00555	0.9887	0.9884
Modified Priddle	0.28036	0.06725	0.00452	0.9908	0.9905

SSE: sum of squares of error; SE: standard error of the residual; MSE: mean squared error; R^2: coefficient of determination; R^2_{adj}: adjusted coefficient of determination; LCL: lower confidence limit; UCL: upper confidence limit.

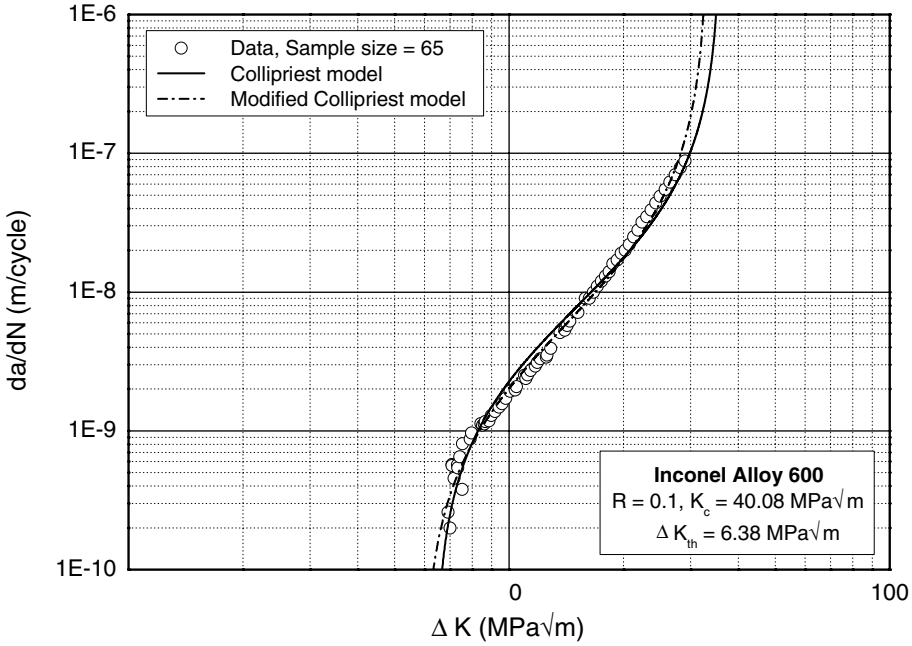

Fig. 4. FCGR curves of Inconel alloy 600, $R = 0.1$, comparison between Collipriest and modified Collipriest models.

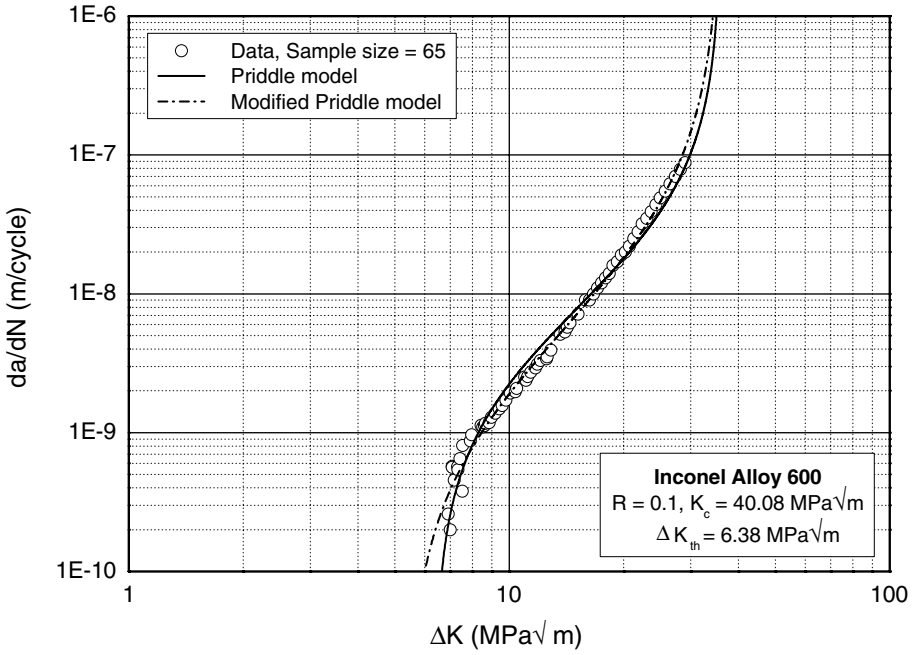

Fig. 5. FCGR curves of Inconel alloy 600, $R = 0.1$, comparison between Priddle and modified Priddle models.

$Q3$ and $Q1$. The horizontal line within the box represents the median. The position of the median relative to the $Q1$ and $Q3$ gives information about the skewness in the middle half of the data. Whiskers are the dashed lines extended from the ends of the box to the adjacent values. The lower adjacent value is defined to be the smallest observation that is greater than or equal to the $Q1 - 1.5 \times IRQ$. The upper adjacent value is defined to be the largest observation that is less than or equal to the $Q3 + 1.5 \times IRQ$. Any observation falls outside the range of the two adjacent values is called an outlier. Notches in the box represent the robust confidence interval around the median and enable an examination of its variability.

Fig. 8 shows side-by-side box plots of the residual data (measured–predicted) of the FCGR models. For all models, the medians of the residuals are similar and nearly equal to zero. Residuals of the Collipriest and Priddle models (Fig. 8a and b) seem to be similar; they appear to be

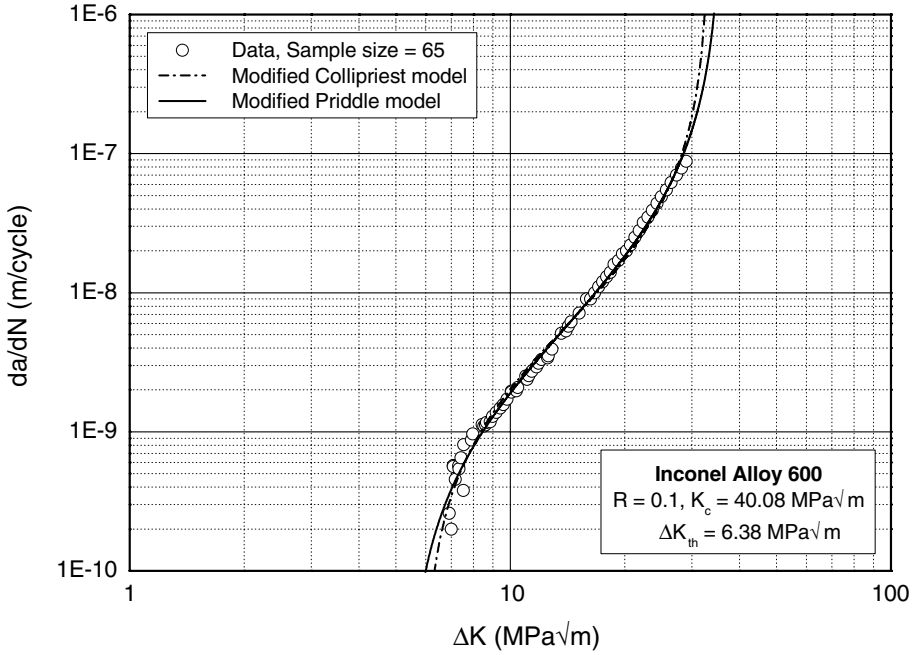

Fig. 6. FCGR curves of Inconel alloy 600, $R = 0.1$, comparison between modified Collipriest and modified Priddle models.

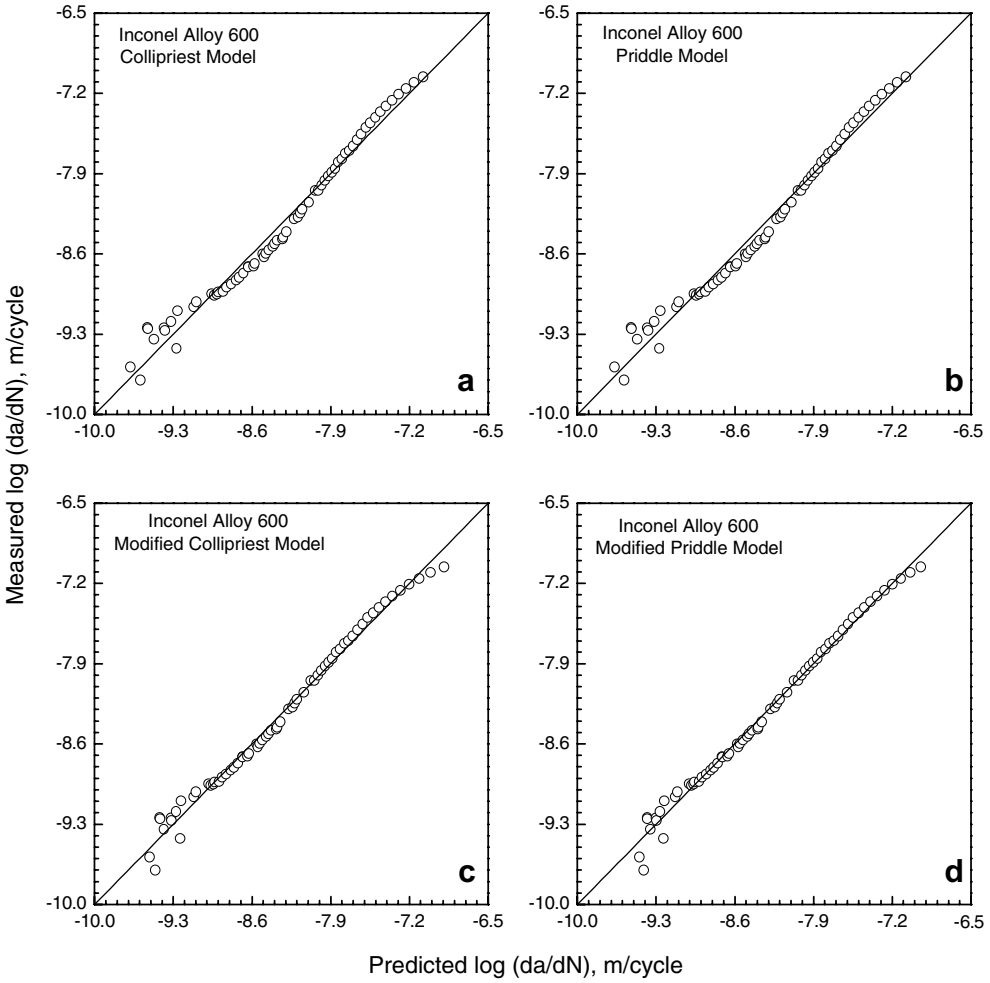

Fig. 7. Measured FCGR values plotted against predictions of FCGR models, Inconel alloy 600, $R = 0.1$.

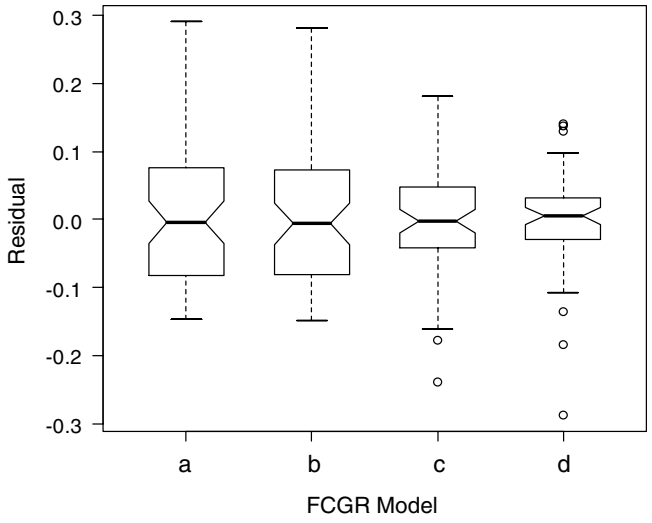

Fig. 8. Box plots for the residual data of FCGR models, Inconel alloy 600, $R = 0.1$, (a) Collipriest model, (b) Priddle model, (c) modified Collipriest model, and (d) modified Priddle model.

skewed to the right because the upper whisker is longer than the lower one. However, the Priddle model provides a slightly better fit to the data due to the smaller range of the upper whisker.

Box plots for the modified Collipriest and modified Priddle models (Fig. 8c and d) indicate that the distribution is symmetric because of the equal-sized whiskers and because the median line nearly lies in the middle of the box. On the other hand, the residual data have some extreme values (outliers) as indicated by the (○) symbols. The extreme negative values indicate that the estimated FCGR curve is conservative for the corresponding measured data points, as seen in Figs. 4 and 5.

The variability in residual data obtained from the modified Collipriest appears much greater than that from the modified Priddle. This is due to the large range of the whiskers and due to the longer length of the box (IQR). Therefore, it can be concluded that the modified Priddle model is the most approximating model to the data.

3.2.3.3. Normal quantile plot. Fig. 9 shows the normal quantile plots (or normal probability plots) for the residuals of the FCGR models. These plots are constructed by plotting the sorted values of the residual against the corresponding theoretical values from the standard normal distribution. The residuals of the Collipriest and Priddle models (Fig. 9a and b) appear to be skewed to the right, since the configuration seems to be a curve with slope increasing from left to right. Plots in Fig. 9(c) and (d)

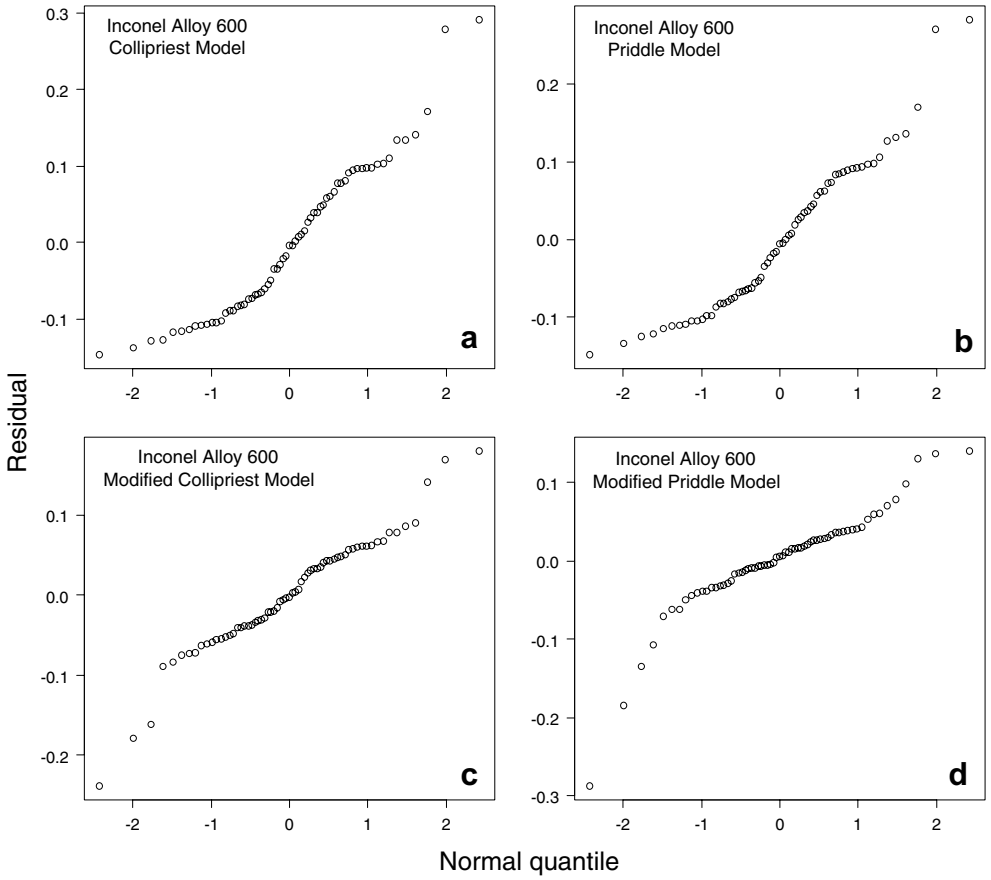

Fig. 9. Normal quantile plots for the residual data of FCGR models, Inconel alloy 600, $R = 0.1$, (a) Collipriest model, (b) Priddle model, (c) modified Collipriest model, and (d) modified Priddle model.

suggest that the residuals of the modified Collipriest and modified Priddle models appear to be normally distributed but contained a small number of outliers. The variability in the body of data for the modified Collipriest is greater than that for the modified Priddle model. Therefore, it may be concluded that the modified Priddle model is the most approximating model to the data.

To assess the model goodness of fit, several commonly used statistical numerical measures such as R^2, R^2_{adj}, SE, and MSE are presented. The R^2 statistic is a poor measure for model validation because adding an extra variable to a model will always increase R^2 even if the variable is completely unrelated to the response variable. The R^2_{adj} statistic adjusts R^2 for the number of parameters in model. A model that maximizes R^2_{adj} may be chosen. Small values of SE and MSE indicate that the model explains the data well. Table 4 suggests that the modified Collipriest and modified Priddle models ($R^2_{adj} \approx 0.99$) are the best approximating models to the data. However, Figs. 7–9 demonstrated that the modified Priddle model provides relatively a better fit than the modified Collipriest.

3.2.4. Information-theoretic criteria and model selection

The least-squares criterion quantifies goodness of fit as the sum of squares of the vertical distances of the data points from the assumed model. That is, the best model for a particular data set is that with the smallest SSE. In fact, it is not simple to compare models with different parameters. The problem is that a more complex model (more parameters) gives more flexibility (more inflection points) for the curve being generated than the curve being defined by a simpler model (fewer parameters). Thereby, the SSE of a more complex model tends to be lower, irrespective of whether the model is the most appropriate one for that data or not.

A model that is too simple cannot capture the regularity in the data; thereby, estimates will be far away from the unknown reality that generated the data (i.e. under-fitting or model bias). A model that is too complex tends to spread the data too thin over too many parameters, resulting in a poor estimate of each parameter (i.e. over-fitting or model variance). It absorbs random noise more easily than a simple model. Simpler models have more bias but less variance; complex models have more variance but less bias [29]. The best model, therefore, is one that provides the right balance between bias and variance. To achieve this, information-theoretic criteria proposed for model selection may be used. Among the various criteria, Akaike Information Criterion (AIC) and Bayesian Information Criterion (BIC) are widely accepted [16–19].

The AIC is an asymptotically unbiased estimator of the expected Kullbach–Leibler (K–L) information [30] lost when a model is used to approximate the underlying process (full reality) that generated the observed data. The K–L information can be interpreted as a "distance" between full reality and a model. Thereby, the best model loses the least information relative to other models in the set. The AIC is given by

$$\mathrm{AIC} = -2\ln(L) + 2K \tag{7}$$

where L is the maximized likelihood and K is the number of estimated parameters in the model plus one (for estimated variance). The first term on the right-hand side represents a lack of fit measure, whereas the second term represents a model complexity measure. In the case of least-squares estimation, the AIC is given by

$$\mathrm{AIC} = N\ln\left(\frac{\mathrm{SSE}}{N}\right) + 2K \tag{8}$$

where N is the number of data points (sample size). When more parameters are added to a model, the first term becomes smaller, whereas the second term becomes larger.

When N is small compared to K for the highest dimensioned model in the set of candidates (as a rough rule of thumb, $N/K < 40$), the use of $\mathrm{AIC_C}$ (Akaike Information Criterion corrected for small samples) is recommended [18]. The $\mathrm{AIC_C}$ is given by

$$\mathrm{AIC_C} = \mathrm{AIC} + \frac{2K(K+1)}{N-K-1} \tag{9}$$

where $2K(K+1)/(N-K-1)$ is a correction term. If N is much larger than K, the numerator of the correction term will be small compared to the denominator and the correction will be tiny. In this case, the AIC or $\mathrm{AIC_C}$ may be used in model selection. For small samples, the correction is matter and the $\mathrm{AIC_C}$ will be used.

Models can only be compared using the AIC or $\mathrm{AIC_C}$ when they have been fitted to exactly the same data set. Within the candidate models, a model minimizing the AIC or $\mathrm{AIC_C}$ should be selected to approximate the underlying process (truth). The use of the $\mathrm{AIC_C}$ rather than AIC is preferred since it is more accurate for small samples and both are very similar for large samples.

Table 5
Model comparison, Inconel alloy 600, $R = 0.1$

Model	K	AIC	$\mathrm{AIC_C}$	Δ	$L(M_i\|D)$	W	R^2_{adj}
Collipriest	3	−294.737	−294.356	50.993	8.45E−12	8.44E−12	0.9789
Priddle	3	−299.536	−299.156	46.193	9.32E−11	9.30E−11	0.9804
Modified Collipriest	4	−332.669	−332.025	13.324	1.28E−03	0.001279	0.9884
Modified Priddle	4	−345.994	−345.349	0	1	0.9987	0.9905

K is the number of parameters in the regression model plus 1 for the variance (σ^2).

A determination of the AIC_C differences (Δ) allows a quick comparison and ranking of candidate models. For the ith model, the Δ_i is given by

$$\Delta_i = AIC_{Ci} - \min AIC_C \quad (10)$$

where min AIC_C is the smallest AIC_C among all candidate models. The Δ of the best approximating model thereby equals zero, while the rest of the models have positive values. The larger the Δ for a model, the less probable is the best approximating model in the candidate set. As a rule of thumb [18], models with $\Delta \leqslant 2$ have substantial support, those with $3 \leqslant \Delta \leqslant 7$ have considerably less support, and models with $\Delta > 10$ have essentially no support.

The likelihood (L) of a model (M_i), given the data (D) is

$$L(M_i|D) = \exp(-0.5\Delta_i) \quad (11)$$

The likelihood of the best model equals unity ($\Delta = 0$) and all other likelihoods are relative to the likelihood of the best model. The Akaike weight for the ith model (W_i) in the set is given as the likelihood of the model divided by the sum of the likelihoods of all of the candidates. The W may be interpreted as the ''probability'' that a model is the best approximation to the reality, given the data. The W for the best model does not equal unity. The smaller is the W, the less plausible the model as the true K–L best model for the data. The evidence ratio of model i versus model j is given by W_i/W_j; this is identical to the ratio of likelihood of model i to that of model j. The ratio W_i/W_j estimates how many times more support the data provide for model i than model j [18].

If two models have similar W scores, but one uses many more parameters than the other, the model with the fewest parameters will be selected. This is because both models fit about equally well, but the simpler is the more parsimonious model.

The AIC can be used to compare both nested and non-nested models, whereas traditional likelihood ratio tests are valid only for nested models. The AIC was used to select the best model from the candidates available since these are non-nested models. Table 5 gives a comparison among the fitting models. Since the modified Priddle shows AIC_C score lower than those for the other models in the set, it is the closest model to the truth.

Based on R^2_{adj} values, Table 5 suggests that the modified Collipriest and modified Priddle models ($R^2_{adj} \approx 0.99$) are the best approximating models to the data. However, an examination of the Δ values shows that the modified Collipriest is very poor relative to the modified Priddle model. Based on the W values, the modified Priddle model is 780 times more likely to be correct. Thereby, it may be concluded that the R^2_{adj} is a poor statistical tool for model selection.

4. Conclusions

Fatigue crack growth rate in Inconel alloy 600 was evaluated in air and at room temperature under constant amplitude loading at a stress ratio of 0.1, using compact tension specimens. Consequently, the collected data were modeled using Collipriest and Priddle models. In addition, these models were modified to obtain a better fit to the data, especially in the near-threshold region. Several commonly used graphical plots and statistical numerical measures were presented to assist the model goodness of fit. The commonly used R^2_{adj} statistic was found to be inefficient for model selection. Then, Akaike information-theoretic criterion was used to select the candidate model that best approximates the real process given the data. The modified Priddle model was found to be the most appropriate model to the observed data.

References

[1] Friend WZ. Corrosion of nickel and nickel-base alloys. New York: Wiley; 1980.
[2] Inconel EL Alloy 600. Aerospace structural metals handbook, vol. IV, 1999.
[3] Crum JR. Major applications and corrosion performance of nickel alloys. In: Corrosion. ASM handbook, vol. 13. ASM; 1992.
[4] Klarstrom DL. Characteristics of nickel and nickel-base alloys. In: Corrosion. ASM handbook, vol. 13. ASM; 1992.
[5] Warke WR. Stress-corrosion cracking. In: Failure analysis and prevention. ASM handbook, vol. 11. ASM; 2002.
[6] Briceno DG, Hernandez AML, Marin MLC. Degradation of Inconel 600 MA steam generator tubes and potential replacement materials. Theor Appl Fract Mech 1994;21:59–71.
[7] James LA. Fatigue-crack propagation behaviour of Inconel 600. Int J Pressure Vessels Piping 1977;5:241–59.
[8] Brog TK, Jones JW, Was GS. Fatigue crack growth retardation inconel 600. Eng Fract Mech 1984;20:313–20.
[9] Damage tolerant design handbook, vol. 2, WL-TR-94-4053, 1994.
[10] Park H-B, Kim Y-H, Lee B-W, Rheem K-S. Effect of heat treatment on fatigue crack growth rate of Inconel 690 and Inconel 600. J Nucl Mater 1996;231:204–12.
[11] Collipriest JE. An experimentalist's view of the surface flaw problem. ASME 1972:43–61.
[12] Collipriest JE, Ehret RM, Thatcher C. Fracture mechanics equations for cyclic growth. NASA technology utilization report, MFS-24447, 1973.
[13] Anderson TL. Fracture mechanics: fundamentals and applications. second ed. CRC Press; 1995.
[14] Ratkowsky DA. Nonlinear regression modeling: a unified practical approach. New York, NY: Marcel Dekker, Inc.; 1983.
[15] Bates DM, Watts DG. Nonlinear regression analysis and its applications. New York: Wiley; 1988.
[16] Akaike H. Information theory as an extension of the maximum likelihood principle. In: Petrov BN, Csaki F, editors. Proceeding of the Second International Symposium on Information Theory. Budapest: Akademiai Kiado; 1973. p. 267–81.
[17] Thelin T, Runeson P. Fault content estimations using extended curve fitting models and model selection. EASE'2000, 4th International Conference on Empirical Assessment & Evaluation in Software Engineering, Keele, England, 2000, pp. 77–96.
[18] Burnham KP, Anderson DR. Model selection and multimodel inference: a practical information-theoretic approach. second ed. Berlin: Springer; 2002.
[19] Posada D, Buckley TR. Model selection and model averaging in phylogenetics: advantages of Akaike information criterion and Bayesian approaches over likelihood ratio tests. Syst Biol 2004;53(5):793–808.
[20] ASTM E8. Standard test methods for tension testing of metallic materials. Annual book of ASTM standards. ASTM; 2001.

[21] ASTM E647. Standard test method for measurement of fatigue crack growth rates. Annual book of ASTM standards. ASTM; 2001.
[22] ASTM E561. Standard practice for *R*-curve determination. Annual book of ASTM standards. ASTM; 2001.
[23] AMS 5540L. Nickel alloy, corrosion and heat resistant, sheet, strip, and plate, 74Ni–15.5Cr–8.0Fe, annealed; 2000.
[24] Paris PC, Erdogan F. A critical analysis of crack propagation laws. J Basic Eng 1963(December):528–34.
[25] Rolfe ST, Barsom JM. Fracture and fatigue control in structures: application of fracture mechanics. Prentice-Hall, Inc.; 1977. p. 224.
[26] Marquardt DW. An algorithm for least squares estimation of parameters. J Soc Ind Appl Math 1963;11:431–41.
[27] Chambers JM, Cleveland WS, Kleiner B, Tukey PA. Graphical methods for data analysis. Duxbury Press; 1983.
[28] Devore JL, Farnum NR. Applied statistics for engineers and scientists. Duxbury Press; 1999.
[29] Pitt MA, Myung IJ. When a good fit can be bad. Trends Cognitive Sci 2002;6:421–5.
[30] Kullbach S. Information theory and statistics. New York: Wiley; 1959.